A Letters Journal Exploring the Frontiers of Physics

December 2016

EPL, **116** (2016) 64004
doi: 10.1209/0295-5075/116/64004

www.epljournal.org

Clustering instability of focused swimmers

Eric Lauga[1(a)] and Francois Nadal[2(b)]

[1] *Department of Applied Mathematics and Theoretical Physics, University of Cambridge - Cambridge CB3 0WA, UK*
[2] *Department of Mechanical, Electrical and Manufacturing Engineering, Loughborough University Loughborough LE11 3TU, UK*

received 28 September 2016; accepted in final form 18 January 2017
published online 9 February 2017

PACS 47.63.Gd – Swimming microorganisms

Abstract – One of the hallmarks of active matter is its rich nonlinear dynamics and instabilities. Recent numerical simulations of phototactic algae showed that a thin jet of swimmers, obtained from hydrodynamic focusing inside a Poiseuille flow, was unstable to longitudinal perturbations with swimmers dynamically clustering (Jibuti L. *et al.*, *Phys. Rev. E*, **90**, (2014) 063019). As a simple starting point to understand these instabilities, we consider in this paper an initially homogeneous one-dimensional line of aligned swimmers moving along the same direction, and characterise its instability using both a continuum framework and a discrete approach. In both cases, we show that hydrodynamic interactions between the swimmers lead to instabilities in density for which we compute the growth rate analytically. Lines of pusher-type swimmers are predicted to remain stable while lines of pullers (such as flagellated algae) are predicted to always be unstable.

Introduction. – A fascinating recent development in soft-condensed-matter physics is the flurry of new results on active matter [1]. Originally motivated by the overdamped limit of swimming microoganisms [2], the physics of active matter also encompasses active gels, driven granular suspensions, filament-motor protein complexes and the cytoskeleton of eukaryotic cells [3].

One of the important issues in active matter research is that of pattern formation and instabilities. Under which conditions does a particular homogeneous, isotropic system remain stable and what parameters govern its transition to a fluctuating, inhomogeneous state?

The question of stability has been the subject of many theory papers in the case of swimming-cell suspensions. Aligned three-dimensional suspensions of swimmers are always unstable to density and orientation perturbations [4–6]. In contrast, homogeneous, isotropic suspensions are linearly unstable to long-wavelengths perturbations in orientation for pushers-type cells (swimming cells propelled from their back, such as flagellated bacteria) but stable for pullers-type cells (cells propelled from their front, such as flagellated algae) [6–8].

Beyond stability, many studies have looked to characterise the nonlinear, collective dynamics of swimming cells, both computationally [9] and experimentally [10], and have shown how collective modes of locomotion could lead to enhanced transport in the surrounding fluid [11–14] and mixing [15], novel rheological characteristics [16,17] and could power synthetic systems [18].

Recently, a numerical study addressed the dynamics of a suspension of phototactic algae, *i.e.*, cells whose direction of motion was set by the presence of an external light source. When present in a pressure-driven (Poiseuille) flow, these swimming cells hydrodynamically focus into a thin jet in the center of the channel (itself a classical result [19]) which was shown to be unstable to longitudinal perturbations with swimmers clustering along the jet [20]. This instability is illustrated in fig. 1(a) and a similar instability was observed numerically in the case of one-dimensional lines of model algae (fig. 1(b)).

As a simple starting point to understand these instabilities, we consider in this paper the problem of an initially homogeneous one-dimensional line of aligned swimmers moving along the same direction. We ignore rotational diffusion (except in the introduction section where the standard theoretical framework is summarised) and, therefore, the swimmers remain aligned, while their one-dimensional density is allowed to vary. We characterise analytically density instabilities using two complementary modelling approaches, namely a continuum framework and a discrete, point-swimmer, framework. In both cases we show

(a) E-mail: e.lauga@damtp.cam.ac.uk
(b) E-mail: francois.nadal33@gmail.com

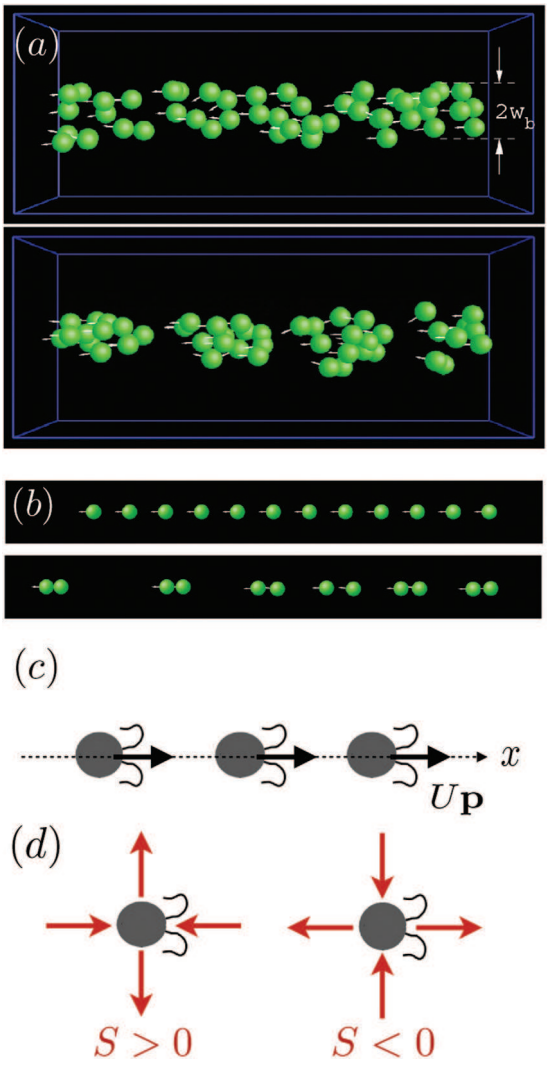

Fig. 1: (Colour online) (a) Clustering instability of phototactic algae from numerical simulations as main motivation for our work [20]; (b) Similar instability arising on a one-dimensional line of swimming algae, which is the precise setup considered in this paper. Reproduced from Jibuti L. *et al.*, *Phys. Rev. E*, **90** (2014) 063019. © 2014, American Physical Society; (c) sketch of the model problem addressed in this paper: a one-dimensional line of swimmers of fixed orientation $\mathbf{p} = \mathbf{e}_x$ swimming with identical speed U in the absence of rotational diffusion; (d) each swimmer acts on the fluid as a stresslet of magnitude S, creating in the swimming frame local flows as illustrated by solid red arrows.

that hydrodynamic interactions between the swimmers are responsible for the clustering and compute the growth rate of the instability. Both approaches give the same results and indicate that the instability arises only for puller-type swimmers such as the algae considered in ref. [20] while pushers are predicted to remain stable.

Continuum framework. – In the first approach, we use the classical continuum framework for suspension of swimming cells [4,21]. The suspension is characterised by a probability distribution function, $\Psi(\mathbf{r}, \mathbf{p}, t)$, for the position $\mathbf{r}$ and orientation $\mathbf{p}$ of the cells. Conservation of probability is written as

$$\frac{\partial \Psi}{\partial t} + \nabla_{\mathbf{r}} \cdot (\dot{\mathbf{r}}\Psi) + \nabla_{\mathbf{p}} \cdot (\dot{\mathbf{p}}\Psi) = D\nabla^2_{\mathbf{r}}\Psi + D_R\nabla^2_{\mathbf{p}}\Psi, \quad (1)$$

where D is a diffusion constant in position and D_R in orientation. The swimmers self-propel with speed U along their direction $\mathbf{p}$ (fig. 1(c)) and are also advected by the flow $\mathbf{u}$ and, thus, we have the relationship

$$\dot{\mathbf{r}} = U\mathbf{p} + \mathbf{u}. \quad (2)$$

The velocity field $\mathbf{u}$ is incompressible, $\nabla_{\mathbf{r}} \cdot \mathbf{u} = 0$, and it satisfies the Stokes equation with a pressure field q,

$$-\nabla_{\mathbf{r}} q + \mu\nabla^2_{\mathbf{r}}\mathbf{u} + \nabla_{\mathbf{r}} \cdot \boldsymbol{\Sigma} = \mathbf{0}, \quad (3)$$

the last term being the active stress due to the active particles, namely the stresslet

$$\boldsymbol{\Sigma} = S\left\langle \mathbf{pp} - \frac{1}{3}\mathbf{1} \right\rangle, \quad (4)$$

where the brackets $\langle\cdot\rangle$ denote orientational average, *i.e.*,

$$\langle\cdot\rangle \equiv \int \Psi(.)\mathrm{d}\mathbf{p}. \quad (5)$$

In eq. (4), the sign of the stresslet strength, S, plays an important role in collective dynamics: $S < 0$ for pushers and $S > 0$ for pullers (see illustration in fig. 1(d)).

In the simulation of ref. [20], the swimmers are phototactic and their swimming orientation is identical and aligned with the line of swimmers. We thus assume here that the swimmers are located on a single line, along the x-direction, and that their orientation is fixed and also along x. We thus look for solutions of the form

$$\Psi = \delta(y)\delta(z)\lambda(x,t)\delta(\mathbf{p} - \mathbf{e}_x), \quad (6)$$

where λ is the one-dimensional density of swimmers along the x-axis. Note that for the particular solution of the form of eq. (6) to be admissible, we ignore diffusion in orientation in what follows as well as diffusion in position in the directions perpendicular to the axis x. Given the fixed orientation, the active stress is given by

$$\boldsymbol{\Sigma} = S\int \Psi\left(\mathbf{e}_x\mathbf{e}_x - \frac{1}{3}\mathbf{1}\right)\mathrm{d}\mathbf{p}, \quad (7)$$

which, using eq. (6), becomes

$$\boldsymbol{\Sigma} = S\delta(y)\delta(z)\lambda(x,t)\left(\mathbf{e}_x\mathbf{e}_x - \frac{1}{3}\mathbf{1}\right). \quad (8)$$

The flow equation becomes

$$\frac{\partial q}{\partial x} = \mu\nabla^2 u_x + \frac{2}{3}S\frac{\partial}{\partial x}\left[\delta(y)\delta(z)\lambda(x,t)\right], \quad (9)$$

$$\frac{\partial q}{\partial y} = \mu\nabla^2 u_y - \frac{1}{3}S\frac{\partial}{\partial y}\left[\delta(y)\delta(z)\lambda(x,t)\right], \quad (10)$$

$$\frac{\partial q}{\partial z} = \mu\nabla^2 u_z - \frac{1}{3}S\frac{\partial}{\partial z}\left[\delta(y)\delta(z)\lambda(x,t)\right], \quad (11)$$

$$0 = \frac{\partial u_x}{\partial x} + \frac{\partial u_y}{\partial y} + \frac{\partial u_z}{\partial z}. \quad (12)$$

In order to make progress, we use Fourier transforms defined for any function $\alpha(\mathbf{x},t)$ of space and time as

$$\alpha(\mathbf{x},t)=\frac{1}{(2\pi)^3}\int e^{i(\mathbf{k}\cdot\mathbf{x})}\hat{\alpha}(\mathbf{k},t)\mathrm{d}\mathbf{k}. \quad (13)$$

We proceed by Fourier-transforming eqs. (9)–(12) in space leading to

$$ik_x\hat{q} = -\mu k^2\hat{u}_x+\frac{2}{3}Sik_x\hat{\lambda}, \quad (14)$$

$$ik_y\hat{q} = -\mu k^2\hat{u}_y-\frac{1}{3}Sik_y\hat{\lambda}, \quad (15)$$

$$ik_z\hat{q} = -\mu k^2\hat{u}_z-\frac{1}{3}Sik_z\hat{\lambda}, \quad (16)$$

$$0 = \mathbf{k}\cdot\hat{\mathbf{u}}. \quad (17)$$

In order to determine the pressure we take the dot product of the $\mathbf{k}$ vector with the first three equations and exploit eq. (17) to get

$$ik^2\hat{q}=Si\hat{\lambda}\left[\frac{2}{3}k_x^2-\frac{1}{3}(k_y^2+k_z^2)\right]=Si\hat{\lambda}\left[k_x^2-\frac{1}{3}k^2\right]. \quad (18)$$

Plugging eq. (18) into eq. (14) then leads to

$$i\frac{k_x}{k^2}S\hat{\lambda}\left[k_x^2-\frac{1}{3}k^2\right]=-\mu k^2\hat{u}_x+\frac{2}{3}Sik_x\hat{\lambda}, \quad (19)$$

which can be solved for $\hat{u}_x$ as

$$\hat{u}_x=\frac{iS\hat{\lambda}}{\mu}\frac{k_x}{k^2}\left(1-\frac{k_x^2}{k^2}\right). \quad (20)$$

In order to close the stability calculation we finally need to write down the conservation of swimmers along the line. In one dimension the conservation of swimmers is written as

$$\frac{\partial\lambda}{\partial t}+\frac{\partial}{\partial x}\left[(U+u_x|_{(x,0,0,t)})\lambda\right]=D\frac{\partial^2\lambda}{\partial x^2}. \quad (21)$$

Note that using the Fourier notation, we can see that

$$u_x|_{(x,0,0,t)}=\frac{1}{(2\pi)^3}\int e^{ik_xx}\hat{u}_x(\mathbf{k},t)\mathrm{d}\mathbf{k}. \quad (22)$$

The base case is a uniform distribution of swimmers, characterised by $\lambda(x,t)=\lambda_0$, so that $\hat{\lambda}=\lambda_0\delta(k_x)$. Note that λ_0 is the inverse of the initial inter-swimmer distance, which we denote by Δ in what follows. From eq. (22) and using eq. (20) we thus see that

$$u_x|_{(x,0,0,t)}=\int e^{ik_xx}\frac{iS\lambda_0\delta(k_x)}{\mu}\left(\frac{k_x}{k^2}-\frac{k_x^3}{k^4}\right)\mathrm{d}\mathbf{k}=0, \quad (23)$$

and, therefore, the uniform concentration is indeed a base state.

We then consider perturbations of this case state, written as $\lambda(x,t)=\lambda_0+\lambda'$, $u_x=u_x'$. The linearisation of eq. (21) around the base state gives

$$\frac{\partial\lambda'}{\partial t}+U\frac{\partial\lambda'}{\partial x}+\lambda_0\frac{\partial}{\partial x}\left[u_x'|_{(x,0,0,t)}\right]=D\frac{\partial^2\lambda'}{\partial x^2}. \quad (24)$$

To get a self-contained equation for λ' we then use the definition of the Fourier integral and rewrite it as

$$\frac{\partial\lambda'}{\partial t}+U\frac{\partial\lambda'}{\partial x}+i\frac{\lambda_0k_x}{(2\pi)^3}\int e^{ik_xx}\hat{u}_x'(\mathbf{k},t)\mathrm{d}\mathbf{k}=D\frac{\partial^2\lambda'}{\partial x^2}. \quad (25)$$

Fourier transforming along the x-direction gives

$$\frac{\partial\hat{\lambda}'}{\partial t}+Uik_x\hat{\lambda}'+\frac{i\lambda_0k_x}{(2\pi)^2}\int\hat{u}_x'(\mathbf{k},t)\mathrm{d}k_y\mathrm{d}k_z=-Dk_x^2\hat{\lambda}'. \quad (26)$$

and then using eq. (20) leads to the final stability relationship

$$\frac{\partial\hat{\lambda}'}{\partial t}+Uik_x\hat{\lambda}'=\frac{Sk_x^2\lambda_0\lambda'}{\mu(2\pi)^2}\int\left(1-\frac{k_x^2}{k^2}\right)\frac{\mathrm{d}k_y\mathrm{d}k_z}{k^2}-Dk_x^2\hat{\lambda}'. \quad (27)$$

Looking for exponentially growing modes of the form $\hat{\lambda}'(k_x,t)=f(k_x)e^{\sigma t}$ and we find a dispersion relation

$$\sigma=-iUk_x+\frac{Sk_x^2\lambda_0}{\mu(2\pi)^2}\int\left(1-\frac{k_x^2}{k^2}\right)\frac{\mathrm{d}k_y\mathrm{d}k_z}{k^2}-Dk_x^2. \quad (28)$$

This dispersion relationship has three terms. The first is a pure traveling mode reflecting the fact that we are in the laboratory frame while the swimmers move with speed U. The third term is diffusive and stabilizing. In contrast, the second term is the one arising from hydrodynamic interactions and is the one leading to instabilities.

We can evaluate the integral in the second term of eq. (28) using cylindrical coordinates, writing $k_\perp^2=k_y^2+k_z^2$, which yields

$$I=\int\frac{1}{k^2}\left(1-\frac{k_x^2}{k^2}\right)\mathrm{d}k_y\mathrm{d}k_z=2\pi\int_{k_{\min}}^{k_{\max}}\frac{k_\perp^3}{(k_\perp^2+k_x^2)^2}\mathrm{d}k_\perp, \quad (29)$$

where the bounds $k_{\min}$ and $k_{\max}$ of the second integral must be specified. We assume for simplicity that the swimmers move in an unbounded space such that the lower bound $k_{\min}$ can be taken equal to zero. The upper bound needs to scale with Δ^{-1} since below the length scale Δ the continuous approach loses its meaning; for simplicity we take it here to be $k_{\max}=\Delta^{-1}$ and making a different choice of the form $k_{\max}=\alpha\Delta^{-1}$ does not affect the main results below.

The integral in eq. (29) can then be calculated exactly and one finds

$$\sigma=-iUk_x+\frac{1}{4\pi}\frac{Sk_x^2}{\Delta\mu}f(k_x\Delta)-Dk_x^2, \quad (30)$$

where the function f is given by

$$f(u)\equiv-\left[\ln\left(\frac{u^2}{1+u^2}\right)+\frac{1}{1+u^2}\right]. \quad (31)$$

To capture the instability, we need to consider only the real part, σ_R, of the right-hand side of eq. (30),

i.e., its last two terms. At small wave numbers, *i.e.*, for wavelength much larger than the initial (mean) distance between swimmers $k_x\Delta \ll 1$, the real part of the growth rate scales as

$$\sigma_R(k_x) \sim -\frac{1}{2\pi}\frac{S}{\mu\Delta^3}(k_x\Delta)^2\ln(k_x\Delta), \tag{32}$$

and diffusion plays no role. A similar result will be obtained below with a discrete approach.

As can be seen from eq. (32), in the case of puller cells with $S > 0$, since the log term is negative, the real part of the growth rate is positive, and long wavelengths are unconditionally unstable. As discussed below, when considering practical situations of real microscopic swimmers, small wavelengths are also unstable, and thus a whole band of wavelengths $[0, \Delta^{-1}]$ is unstable, a result in line with Jibuti's simulations [20]. Conversely, for negative values of S, so-called pusher cells, the growth rate is always negative and the system is always stable, also in agreement with Jibuti's results.

Discrete framework. – We now consider a second, complementary, modelling approach for the same problem.

Specifically, we model the three-dimensional swimmers as discrete moving stresslets located on a uniform one-dimensional lattice of spacing Δ. Due to the long-range nature of the hydrodynamic interactions, we include the flow created by all other swimmers when computing the velocity of a given swimmer. The swimmers are equally spaced on the x-axis and we wish to assess the stability of such a situation. In the reference frame moving with speed U along the x-axis, the swimmers are motionless if the situation is unperturbed. We then subject the homogenous line to a harmonic perturbation of wave number $k_x = 2\pi/(p\Delta)$, where p a positive integer, such that each individual swimmer is shifted from its equilibrium position by a small quantity $\epsilon_n \equiv \varepsilon\cos(k_x\, n\Delta) = \varepsilon\cos(2\pi n/p)$ (see notation in fig. 2). Since the wavelength of the perturbation needs to be larger than 2Δ, the wave vector is bounded by π/Δ.

A swimmer located at $\mathbf{r}_0$ generates its own flow given by a force dipole

$$\boldsymbol{u}^d(\mathbf{r}-\mathbf{r}_0) = \boldsymbol{S}(\mathbf{p}):\boldsymbol{\nabla}\boldsymbol{\mathcal{G}}(\mathbf{r}-\mathbf{r}_0), \tag{33}$$

where $\boldsymbol{S}(\mathbf{p}) = S\,\mathbf{pp}$ and $\boldsymbol{\mathcal{G}}(\mathbf{r}) = (\mathbf{1}+\mathbf{rr})/8\pi\mu r$ is the stokeslet (point force) solution. All the dipoles have the same fixed orientation and are subject to the flow generated on the x-axis ($y = z = 0$) by all other swimmers. The x-component of the velocity field, eq. (33), reduces to

$$u^d(x-x_0) = -\frac{S}{4\pi\mu}\frac{x-x_0}{|x-x_0|^3}. \tag{34}$$

In the absence of inertia, the dynamics of swimmer No. n is governed by the evolution of its perturbation,

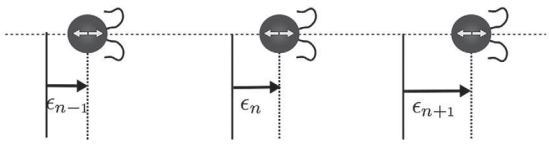

Fig. 2: Discrete homogeneous one-dimensional line of swimmers. In the frame moving with the swimming speed of the cells, the perturbation distance to the equilibrium steady position of each swimming, x_n, is denoted by ϵ_n.

away from the equilibrium position, ϵ_n, which follows thus

$$\dot{\epsilon}_n = \sum_{q>1}\left[u^d(x_n - x_{n-q}) + u^d(x_n - x_{n+q})\right], \tag{35}$$

where the infinite sum includes interactions with all swimmers. The first term on the right-hand side of eq. (35) can be expanded to first order in $\epsilon_n - \epsilon_{n-q}$ since $x_n - x_{n-q} = \Delta + \epsilon_n - \epsilon_{n-q}$ with $(\epsilon_n - \epsilon_{n-q})/\Delta \ll 1$, and one gets at first order

$$u^d(x_n - x_{n-q}) = -\frac{S}{4\pi\mu}(q\Delta)^{-2}\left(1 - 2\frac{\epsilon_n - \epsilon_{n-q}}{q\Delta}\right), \tag{36}$$

with a similar result for $u^d(x_n - x_{n+q})$. Introducing these expansions in eq. (35) leads to the equation which governs the evolution of the ϵ_n in time,

$$\dot{\epsilon}_n = -\frac{S}{4\pi\mu}\sum_{q>1}\frac{1}{(q\Delta)^3}(\epsilon_{n+q} + \epsilon_{n-q} - 2\epsilon_n). \tag{37}$$

Note that this equation is valid in both the laboratory frame or the frame moving with the swimming speed U.

The perturbation in displacement ϵ_n (which "follows" the global displacement of the assembly at speed U) can be considered as a propagative wave in the laboratory frame, so that we consider a discrete perturbation of the form

$$\epsilon_{n\pm q} = \varepsilon\,\mathrm{e}^{\tilde{\sigma}t}\mathrm{e}^{-\mathrm{i}}[k_x(n\pm q)\Delta - \omega t)], \quad \text{with } \omega = k_x U. \tag{38}$$

When introduced in eq. (37), this leads to the dispersion relationship which provides the discrete growth rate $\tilde{\sigma}(k_x)$, and one finds the infinite sum

$$\tilde{\sigma}(k_x) = -\mathrm{i}Uk_x + \frac{2}{\pi}\frac{S}{\mu\Delta^3}\sum_{q>1}\frac{\sin^2(qk_x\Delta/2)}{q^3}. \tag{39}$$

Here again, we see clearly from eq. (39) that if $S < 0$ (pushers) the system is predicted to be stable while a line suspension of pullers ($S > 0$) is always unstable.

To address the behaviour at long wavelengths, we rewrite the real part $\tilde{\sigma}_R$ of the discrete growth rate, the second term on the right-hand side of eq. (39), in the following form:

$$\tilde{\sigma}_R(k_x) = \frac{1}{2\pi}\frac{S}{\mu\Delta^3}(k_x\Delta)^2\sum_{q>1}\frac{\sin^2(qk_x\Delta/2)}{(qk_x\Delta/2)^3}\,\frac{k_x\Delta}{2}. \tag{40}$$

The sum in eq. (40), which has the form of a discrete integral, is bounded as follows:

$$\int_{k_x\Delta/2}^{\infty} \frac{\sin^2 u}{u^3}\,\mathrm{d}u < \sum_{q>1} \frac{\sin^2(qk_x\Delta/2)}{(qk_x\Delta/2)^3}\,\frac{k_x\Delta}{2} < \mathrm{sinc}^2(k_x\Delta/2) + \int_{\bar{k}_x/2}^{\infty} \frac{\sin^2 u}{u^3}\,\mathrm{d}u. \quad (41)$$

Given that the integral in both right and left bounds of the previous double inequality scales as $-\ln k_x\Delta$ for $k_x\Delta \to 0$, one obtains the scaling of σ_R at small wave numbers, namely

$$\tilde{\sigma}_R(k_x) \sim -\frac{1}{2\pi}\frac{S}{\mu\Delta^3}(k_x\Delta)^2 \ln(k_x\Delta), \quad (42)$$

which is exactly the same relationship as the one obtained in the continuum limit, eq. (32).

Discussion. – The spatial organisation of active matter under the combined effects of external Poiseuille flows and physical taxis (such as magnetotaxis or phototaxis) has been the subject of recent numerical and experimental studies [20,22,23]. The interplay between hydrodynamic effects and physical taxis classically results in a focusing of the swimmers close to the axis of the channel [19], the radial density profile being determined by the competition between the swimming-enhanced diffusivity of the swimmers and the amplitudes of external forcing.

In this paper, we examined theoretically the linear stability of swimmers along one-dimensional clusters from both a continuum and discrete perspectives. The continuum approach, performed in Fourier space, leads to a stability condition involving two competing terms coming from hydrodynamic interactions and diffusion, respectively.

At small $k_x\Delta$, both modelling approaches provide a real part of the growth rate scaling as $\sigma_R(k_x) \sim -(1/2\pi)[S/(\mu\Delta^3)](k_x\Delta)^2 \ln(k_x\Delta)$. In this limit diffusion plays no role —a result is in fact true, with very good approximation, for all wave numbers. To see this, we take D/Δ^2 as a typical timescale and denoting by $\bar{k}_x$ the dimensionless product $k_x\Delta$, the real part σ_R of the growth rate obtained in the continuum limit can be rewritten in the following dimensionless form:

$$\bar{\sigma}_R(\bar{k}_x) = \bar{k}_x^2\left[\bar{S}\, f(\bar{k}_x) - 1\right], \quad (43)$$

where $\bar{\sigma}_R = \Delta^2\sigma_R/D$ and $\bar{S} = (1/4\pi)[S/(D\Delta\mu)]$. For microscopic swimmers of size $a = 1\,\mu$m separated by an initial distance $\Delta/a = 2$ and propelled in water ($\mu = 10^{-3}\,\mathrm{Pa}\cdot\mathrm{s}$) by an individual stresslet of $S = 1\,\mathrm{pN}\cdot\mu\mathrm{m}$, and writing $D\mu = k_BT/6\pi a$, where k_B and T refer to the Boltzmann constant and the temperature (300 K), one obtains the dimensionless value $\bar{S} \simeq 181$. Given the typical value of the dimensionless function f, one obtains that the diffusive term in eq. (43) can basically always be neglected and with a good approximation we can write

$$\sigma_R(k_x) \simeq \frac{1}{4\pi}\frac{S}{\mu\Delta^3}\,(k_x\Delta)^2\, f(k_x\Delta). \quad (44)$$

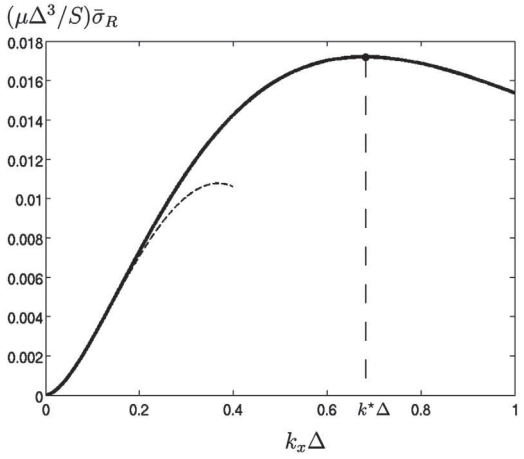

Fig. 3: Dimensionless real part of the growth rate as a function of the dimensionless wave number, in the large-$\bar{S}$ limit, eq. (44). The dashed lines correspond to the improved small $k_x\Delta$ scaling $\sigma_R(k_x) \simeq -(1/2\pi)[S/(\mu\Delta^3)](k_x\Delta)^2\,[\ln(k_x\Delta) + 1/2]$ obtained by taking into account the constant in the Taylor expansion of the function f.

The real part of the growth rate, non-dimensionalised as $S/(\mu\Delta^3)$, is plotted in the large-$\bar{S}$ limit (where diffusion is negligible) as a function of the dimensionless axial wave number, $k_x\Delta$, in fig. 3, for positive values of the stresslet strength S (*i.e.*, in the unstable case of pullers). All wavelengths $k_x\Delta \in [0, 1]$ are seen to be unstable. Furthermore, a most unstable wavelength $k^\star\Delta \approx 0.68$ is obtained. Considering, however, the small difference between the growth rate at $k^\star\Delta$ and at $k_x\Delta = 1$, no real emergence of the most unstable wavelength $\lambda^\star = 2\pi/k^\star$ should be expected experimentally. This is consistent with the "pairing" scenario depicted by Jibuti *et al.* in [20]. It is likely that this pairing would continue in sequence, with swimmer pairs, which also act at pullers, pairing up, eventually leading to one big cluster.

The physical mechanism leading to the instability captured in our paper is in fact quite elementary, and can be captured by considering the line of swimmers sketched in fig. 2. Puller cells induce attractive flows along their swimming axis with a magnitude which increases as one gets closer to the cell (fig. 1(d)). In contrast, pushers induce repulsive flows, also with a magnitude increasing near the cell (fig. 1(d)). Consider a situation where the location of the middle cell in fig. 2 is perturbed to its right. If the cells are pushers, the repulsion with its neighbour on the right increases while the repulsion with the cell on the left decreases, and the cell returns to its original location, indicating stability. If, in contrast, the cells are pullers, the attraction toward the cell on the right increases, and the

attraction with the left cell on the left decreases, leading to an amplification of the original perturbation, and an unstable situation. As a simple analogy, the instability of a line of pullers is thus similar to the instability of a line of point charges with alternating signs where, while the periodic lattice is a fixed point, any perturbation to it is unstable.

While our theoretical predictions agree with the numerical results obtained in ref. [20] showing a jet instabilities for pullers in the absence of diffusion, we note that, in contrast, a recent experimental realisation of focused puller suspensions (specifically, the green alga *Chlamydomonas*) did not display such axial clustering [23]. The origin of this discrepancy could for instance come from the existence of a threshold in flow intensity such as the one observed in ref. [22] for magnetotactic focusing. Indeed the jet pearling transition in ref. [22] was obtained as soon as the value of the flow intensity exceeds a critical value (for a fixed external magnetic field). Another possible source of discrepancy could come from our assumption to model the swimmer as a steady puller. *Chlamydomonas* is a puller on average but in fact oscillates between instantaneous pusher and puller behaviours [24], potentially interfering with the development of an instability.

A simple extension of the situation considered in the present paper would be a configuration in which the direction of swimming is perpendicular to the line of swimmers. In this case, one expects pushers to be unstable while pullers would remain stable. Another extension would focus on an axisymmetric situation in which a cylindrical blob of co-swimmers could be perturbed, or on multiple parallel lines of swimmers. Such analysis would be closer to the experiment in ref. [22] and would be a step further towards the full modelling of instabilities of convected active suspensions subject to physical taxis.

* * *

This work was funded in part by the European Union through a Marie Curie CIG Grant and an ERC consolidator grant to EL.

REFERENCES

[1] Ramaswamy S., *Annu. Rev. Condens. Matter Phys.*, **1** (2010) 323.
[2] Lauga E. and Powers T. R., *Rep. Prog. Phys.*, **72** (2009) 096601.
[3] Marchetti M., Joanny J., Ramaswamy S., Liverpool T., Prost J., Rao M. and Simha R. A., *Rev. Mod. Phys.*, **85** (2013) 1143.
[4] Simha R. A. and Ramaswamy S., *Phys. Rev. Lett.*, **89** (2002) 058101.
[5] Saintillan D. and Shelley M. J., *Phys. Rev. Lett.*, **99** (2007) 058102.
[6] Saintillan D. and Shelley M. J., *Phys. Rev. Lett.*, **100** (2008) 178103.
[7] Hohenegger C. and Shelley M. J., *Phys. Rev. E*, **81** (2010) 046311.
[8] Koch D. L. and Subramanian G., *Annu. Rev. Fluid Mech.*, **43** (2011) 637.
[9] Hernandez-Ortiz J. P., Stoltz C. G. and Graham M. D., *Phys. Rev. Lett.*, **95** (2005) 204501.
[10] Sokolov A. and Aranson I. S., *Phys. Rev. Lett.*, **109** (2012) 248109.
[11] Wu X. L. and Libchaber A., *Phys. Rev. Lett.*, **84** (2000) 3017.
[12] Valeriani C., Li M., Novosel J., Arlt J. and Marenduzzo D., *Soft Matter*, **7** (2011) 5228.
[13] Jepson A., Martinez V. A., Schwarz-Linek J., Morozov A. and Poon W. C. K., *Phys. Rev. E*, **88** (2013) 041002.
[14] Kasyap T. V., Koch D. L. and Wu M., *Phys. Fluids*, **26** (2014) 081901.
[15] Pushkin D. O. and Yeomans J. M., *Phys. Rev. Lett.*, **111** (2013) 188101.
[16] Chen D. T. N., Lau A. W. C., Hough L. A., Islam M. F., Goulian M., Lubensky T. C. and Yodh A. G., *Phys. Rev. Lett.*, **99** (2007) 148302.
[17] Sokolov A. and Aranson I. S., *Phys. Rev. Lett.*, **103** (2009) 148101.
[18] Sokolov A., Apodaca M. M., Grzybowski B. A. and Aranson I. S., *Proc. Natl. Acad. Sci. U.S.A.*, **107** (2010) 969.
[19] Pedley T. J. and Kessler J. O., *Annu. Rev. Fluid Mech.*, **24** (1992) 313.
[20] Jibuti L., Qi L., Misbah C., Zimmermann W., Rafaï S. and Peyla P., *Phys. Rev. E*, **90** (2014) 063019.
[21] Saintillan D. and Shelley M. J., *C. R. Phys.*, **14** (2013) 497.
[22] Waisbord N., Lefvre C., Bocquet L., Ybert C. and Cottin-Bizonne C., *Phys. Rev. Fluids*, **1** (2016) 053203.
[23] Martin M., Barzyk A., Bertin E., Peyla P. and Rafai S., *Phys. Rev. E*, **93** (2016) 051101.
[24] Klindt G. S. and Friedrich B. M., *Phys. Rev. E*, **92** (2015) 063019.